

# Associative Fear Learning Enhances Sparse Network Coding in Primary Sensory Cortex

Amos Gdalyahu,<sup>1,2,3,\*</sup> Elaine Tring,<sup>1,2,3</sup> Pierre-Olivier Polack,<sup>4</sup> Robin Gruver,<sup>1</sup> Peyman Golshani,<sup>2,3,4</sup> Michael S. Fanselow,<sup>2,3,5,6</sup> Alcino J. Silva,<sup>1,2,3,5,6</sup> and Joshua T. Trachtenberg<sup>1,2,3</sup>

<sup>1</sup>Department of Neurobiology

<sup>2</sup>Brain Research Institute

<sup>3</sup>Integrative Center for Learning and Memory

<sup>4</sup>Department of Neurology

<sup>5</sup>Department of Psychology

<sup>6</sup>Department of Psychiatry and Biobehavioral Sciences

University of California Los Angeles, Los Angeles, CA 90095, USA

\*Correspondence: amos.gdalyahu@gmail.com

<http://dx.doi.org/10.1016/j.neuron.2012.04.035>

## SUMMARY

Several models of associative learning predict that stimulus processing changes during association formation. How associative learning reconfigures neural circuits in primary sensory cortex to “learn” associative attributes of a stimulus remains unknown. Using 2-photon *in vivo* calcium imaging to measure responses of networks of neurons in primary somatosensory cortex, we discovered that associative fear learning, in which whisker stimulation is paired with foot shock, enhances sparse population coding and robustness of the conditional stimulus, yet decreases total network activity. Fewer cortical neurons responded to stimulation of the trained whisker than in controls, yet their response strength was enhanced. These responses were not observed in mice exposed to a nonassociative learning procedure. Our results define how the cortical representation of a sensory stimulus is shaped by associative fear learning. These changes are proposed to enhance efficient sensory processing after associative learning.

## INTRODUCTION

Neural responses in primary sensory cortices encode the physical attributes of a stimulus with considerable precision. Additionally, these neural responses can reflect a large number of experience-dependent contextual attributes of a stimulus (Meyer et al., 2010; Shuler and Bear, 2006; Zhou et al., 2010) including those that reflect its behavioral significance (Polley et al., 2006; Recanzone et al., 1993; Rosselet et al., 2011; Siucinska and Kossut, 1996; Weinberger, 2004).

On the local network level, neuronal responses to a stimulus are both redundant and sparse (Houweling and Brecht, 2008; Kerr et al., 2007; O'Connor et al., 2010; Olshausen and Field, 2004). Redundancy, in which the total number of spikes elicited by a sensory stimulus exceeds the number needed for sensory

perception (Houweling and Brecht, 2008; Huber et al., 2008; O'Connor et al., 2010), permits fault-tolerant coding in cortical networks, which have characteristically high response variability. However, redundant coding increases the metabolic load on the system. This higher metabolic load can be reduced by employing a number of strategies known as “sparse coding” (Willmore et al., 2011). While individual neurons can fire at high instantaneous frequencies, particularly in primary sensory cortices, the maximum sustainable average firing rate has been estimated to be between 1 and 4 Hz (Attwell and Laughlin, 2001). To achieve high instantaneous firing rates while maintaining low average firing rates, the cortex can optimize the fraction of neurons responding when the stimulus is presented (sparse population coding) and/or can optimize how frequently a single neuron responds when the stimulus is presented  $n$  times (lifetime sparseness, or fidelity as used hereafter) (Willmore et al., 2011). Sparse coding optimizes the information per spike while minimizing mean firing rate and redundancy and, thus, minimizes metabolic load as a function of information (Vinje and Gallant, 2000).

Network models show that sparse internal representation facilitates the storage of learned associations, and cortical response sparsification may emerge as associations are learned (Chalupa and Werner, 2003). To examine the relationship between cortical sparsification and associative learning we carried out three sets of experiments. First, we developed a variant of fear conditioning in freely exploring mice in which whisker stimulation (our conditional stimulus [CS]) was either paired or explicitly unpaired with foot shock. Second, we examined how learning the association between the CS and the shock affected subsequent encoding of the CS using *in vivo* calcium imaging. We measured population sparse coding, fidelity, and response strength. Third, to examine if our results were specific to associative learning, we measured the nonassociative effects of stimulus exposure on the population response.

## RESULTS

### Mice Learn to Associate Passive Whisker Stimulation with Shock

The primary somatosensory “barrel” cortex receives tactile information from the whiskers on the facial mystacial pad. This

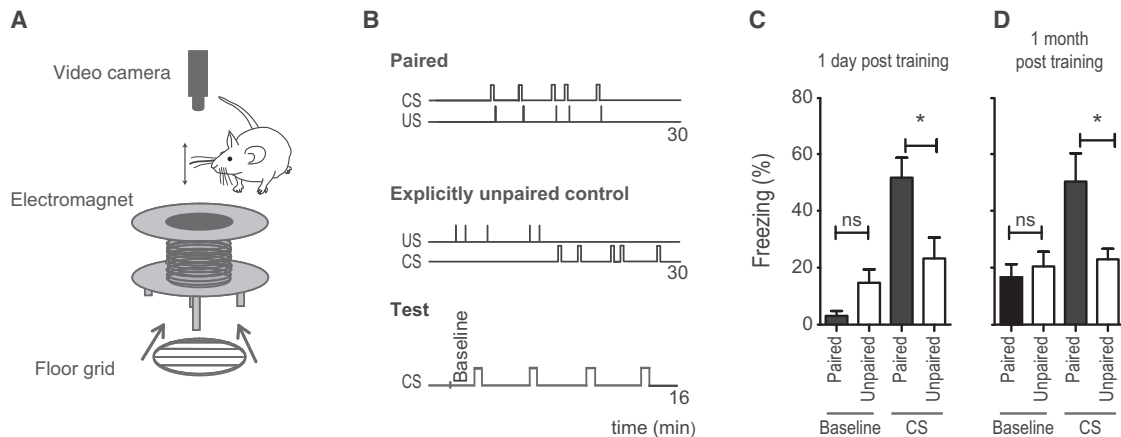


**Figure 1. Fear Conditioning by Passive Whisker Stimulation**

(A) Schematic diagram showing the electromagnet used to passively deflect a whisker, the floor grid used to deliver foot shock, and the camera used to track movement using FreezeFrame software. The mouse would be placed inside the bore of the magnet.  
 (B) Schematic diagram showing the order and timing of the CS and US in paired and unpaired training procedures and at the time of testing.  
 (C and D) Measurements of freezing in paired (black bars) and unpaired (open bars) conditioned mice during baseline and during CS, taken 1 day (C) or 1 month (D) after training; (ns non significant, \* $p < 0.05$ . Statistical analysis Student's  $t$  test. Plots are mean  $\pm$  SEM).  
 See also [Movie S1](#).

system has been exploited in restrained animals to study cortical plasticity induced by Pavlovian fear conditioning (Das et al., 2001; Galvez et al., 2006, 2007; Siucinska and Kossut, 1996), and in freely moving mice to induce associative eye blink conditioning (Galvez et al., 2009). For our studies, we first determined whether freely exploring mice learn Pavlovian fear conditioning where whisker stimulation is used as a CS.

Passive whisker stimulation in freely behaving mice was accomplished by gluing a small metal grain to a specific whisker and placing the mouse in the bore of an electromagnet (7.7 mT) large enough to permit free exploration (Melzer et al., 1985) (Figure 1A). In mice conditioned to associate whisker stimulation with shock, 30 s of whisker stimulation at 8 Hz immediately preceded a single 0.6 mA, 1.5 s foot shock (paired group); this pairing was repeated five times, with a mean interval of 3 min between pairings, in a single day (Figure 1B top). To control for exposure to these two sensory stimuli, a second group received the same stimuli but explicitly unpaired (unpaired control; Figure 1B middle). Hereafter, we refer to the foot shock as the unconditional stimulus, or US.

CS-elicited freezing was examined the following day. To avoid any confounding influence of context-elicited freezing, we tested the mice in a novel context. Because cued-fear memories are context independent (Kim and Fanselow, 1992), this strategy revealed only fear behaviors elicited by the CS and not by the context. Four conditional stimuli were presented (Figure 1B, bottom, "Test") and the amount of time spent motionless (freezing) during each CS was measured and averaged as a behavioral indication of fear (Fanselow and Bolles, 1979). Paired mice ( $n = 12$ ) froze significantly more than explicitly unpaired control mice ( $n = 12$ ) during testing (Figure 1C,  $p < 0.05$ ), demonstrating a learned association between the CS and the US in which the CS triggers fear. An example movie showing freezing during testing is shown in [Movie S1](#) (available

online). This learned association was evident even one month later, when whisker stimulation still induced a 3-fold increase in freezing relative to baseline ( $n = 8$ ) and a significant increase compared to explicitly unpaired controls (Figure 1D,  $n = 9$ ,  $p < 0.05$ ), revealing a long-term memory of the association (see also Gale et al., 2004).

We next examined if the fear response could be evoked by stimulation of either an adjacent or distant, untrained whisker. We found no generalization to a distant, untrained whisker (Figure 2A, compare "CS: Paired trained" with "CS: Paired remote"; paired  $n = 7$ , unpaired  $n = 7$ ) but did find generalization to an adjacent whisker (Figure 2B, compare "CS: Paired trained" with "CS: Paired adjacent"; paired  $n = 6$ , unpaired  $n = 5$ ). This is consistent with a former study in which rats were trained to use a single whisker to decide whether to cross a gap. The rats generalized the learning to an adjacent whisker but not to a remote whisker (Harris et al., 1999).

We then checked another dimension of generalization—whether the behavior could be evoked by stimulating the whisker at a frequency that is different from that used during training. We found that mice that had been trained at 8 Hz also froze when tested at 33 Hz, indicating that the fear response generalizes to other stimulus frequencies (Figure 2C, paired  $n = 7$ , unpaired  $n = 7$ ).

### Associative Fear Learning Enhances Sparse Population Coding

Does the learned CS-US association affect subsequent encoding of the CS in primary sensory cortex? To examine this we used 2-photon in vivo imaging to measure evoked responses of networks of cortical neurons bulk loaded with the calcium-sensitive fluorescent dye OGB-1 (Garaschuk et al., 2006; Stosiek et al., 2003). Intrinsic-signal imaging (Grinvald et al., 1986) was used to target dye injections to the cortical "barrel" column in

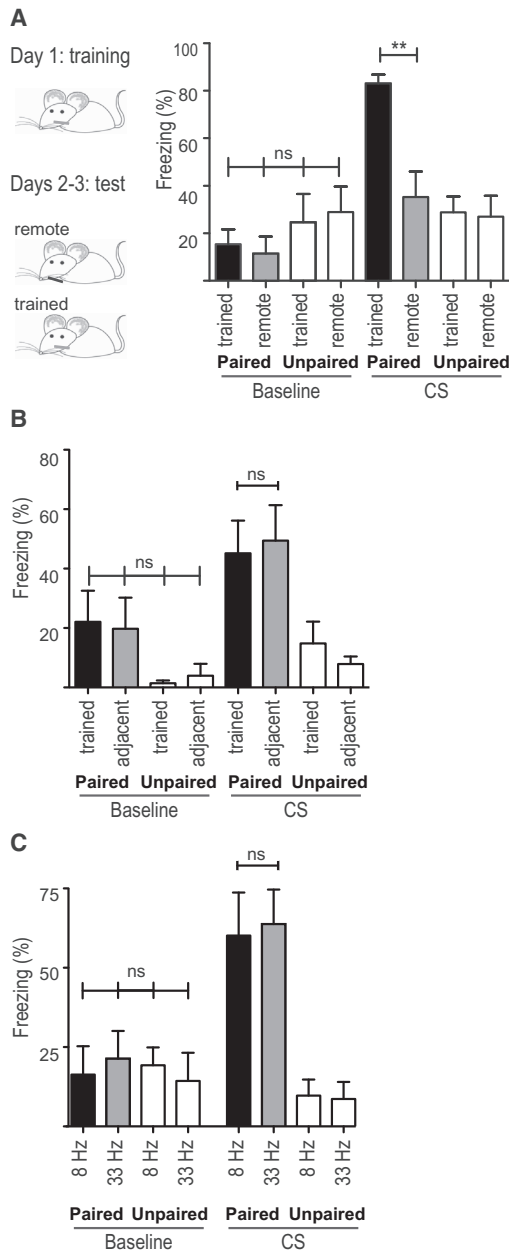


**Figure 2. Measures of Fear Generalization**

(A and B) Mice were exposed to five foot shocks that were either paired or explicitly unpaired with whisker stimulation. (A) The following 2 days the same mice were tested twice, 1 day on the trained whisker (black bars) and the next on a remote, untrained whisker (gray bars). The order of testing was randomized such that half were tested on the first day using the trained whisker and the other half using the remote whisker. Note the absence of generalization to the remote, untrained whisker. (B) The same training paradigm as in (A) was used, but mice were tested on an adjacent, untrained whisker (gray bars). Note the generalization of the fear response to stimulation of the adjacent whisker.

(C) Mice were trained as in (A) and tested on the trained whisker twice: at the trained frequency (8 Hz; black bars) and a remote frequency (33 Hz; gray bars). Note the generalization of the fear response to the higher stimulation frequency. ns, non significant. \*\* $p < 0.01$ . Statistical analysis: one-way ANOVA followed by Tukey's post hoc test. Plots are mean  $\pm$  SEM.

primary somatosensory cortex that represented the whisker that had been stimulated during training (Figure 3A). Measures were made of the fraction of neurons in the network that responded to whisker stimulation, the response magnitude of each imaged neuron, and the fidelity of neural responses across stimulus trials. For each imaging field, neural responses were imaged to ten whisker stimulations spaced 10 s apart. The analyses of changes in fluorescence were restricted to a 2 s window immediately following the onset of whisker stimulation. A total of 816 cells were imaged in seven fear-conditioned mice, and 833 cells in six explicitly unpaired control mice.

Cortical networks are spontaneously active, and this spontaneous activity must be considered when defining evoked responses. To examine spontaneous activity we measured changes in fluorescence in a 2 s time window immediately following each of ten sham whisker stimulations delivered with the same temporal pattern as during actual trials (Figure 3B and Movie S2). We used the resulting statistics of spontaneous activity for two purposes: (1) to examine if associative fear learning affected spontaneous activity, and (2) to define thresholds of response magnitude (Figure 3C) and fidelity (Figure 3D) above which a neuron was considered responsive in subsequent trials with an actual stimulus. Here, mean response magnitude refers to the average fluorescent change across all ten sham stimuli, and fidelity refers to the number of sham trials out of ten that were temporally coincident with a given neuron's spontaneous activity (see Experimental Procedures). Importantly, there were no significant differences in spontaneous activity between paired and explicitly unpaired groups, as measured by mean response magnitude (Figure 3C: paired  $1.17\% \pm 0.06\%$ ; unpaired  $1.16\% \pm 0.03\%$  dF/F,  $p = 0.14$ ), mean response fidelity (Figure 3D paired 1.61; unpaired 1.66,  $p = 0.48$ ) and network synchrony (Ch'ng and Reid, 2010; Golshani et al., 2009) (Figure 3E, two-way ANOVA training effect  $F[1,320] = 1.4$ ,  $p = 0.24$ ). The values of spontaneous response magnitude (Figure 3C), and fidelity (Figure 3D) derived from sham stimuli were then used to determine the threshold for defining with 95% confidence whether a neuron was actually responding to whisker stimulation or simply happened to be spontaneously active at the moment of whisker stimulation. For magnitude of response (dF/F), the 95% cutoff in paired mice was a 3.2% increase in fluorescence above baseline, and for explicitly unpaired mice was 2.7% above baseline (see gray shading in Figure 3C). For fidelity, the 95% cutoff was 4; that is, only 5% of cells were spontaneously active during the sham stimulus more than four out of ten trials (gray shading in Figure 3D). Using these thresholds, neurons could be confidently defined as responsive based on their mean response magnitude or based on the fidelity of their response.

To determine whether associative learning impacts network coding of the CS we imaged cortical responses evoked by stimulation of the trained whisker (Figure 4 and Movie S3). The fraction of responding neurons was measured in two ways because learning could change the fraction of neurons that respond to a single stimulus, or change the fraction of neurons recruited across trials, or both. This is due to the fact that trial-to-trial response variability is high in cortical networks, and thus many neurons that can encode a given stimulus often do not respond

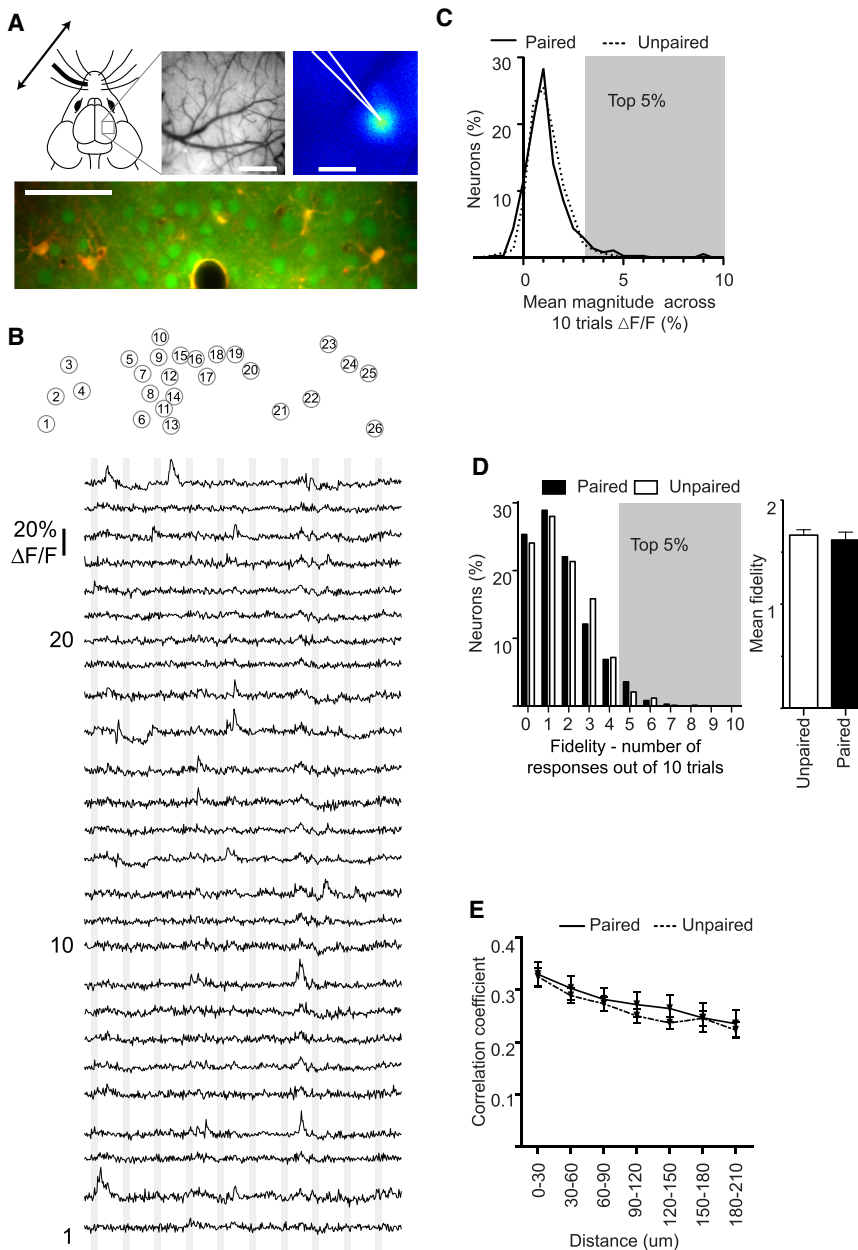


**Figure 3. Spontaneous Activity Is Unchanged by Associative Fear Learning**

(A) Intrinsic-signal imaging was used to identify the trained barrel and vascular landmarks were used to guide OGB-1 loading. An example image of the pial vasculature (top middle) and intrinsic response (top right) are shown. A typical image of labeled cortical neurons, imaged in vivo with 2-photon excitation, is shown in the lower panel. OGB-1 labeling is green; SR101 labeling, which labels astrocytes, is red and the overlap is yellow. Scale bars: vascular and intrinsic maps, 500  $\mu$ m; calcium image, 50  $\mu$ m.

(B) Example traces of spontaneous fluorescent changes in OGB-1 labeled neurons in layer 2/3. (Top) Each circle delineates a single neuron in the image in (A). Each neuron is assigned a number. (Bottom) Change in fluorescence for each of the 26 cells identified above. The vertical gray lines indicate the timing of each sham whisker stimulation. Each trace is 120 s.

(C) Percentage of neurons as a function of mean magnitude of fluorescent change time-locked to a sham stimulus; dashed line indicates unpaired mice, solid line indicates paired mice.

(D) (left) Percentage of neurons as a function of their fidelity—the number of times their spontaneous activity was time-locked to the sham stimuli. (right) Mean fidelity of spontaneous events for each group averaged across all ten sham stimuli. White bars indicate unpaired mice; black bars indicate paired mice.

Gray shadings in (C) and (D) delineate the top 5% of neurons whose spontaneous activity was time-locked to a sham stimulus. This was subsequently used as a threshold to define evoked responsive neurons with 95% confidence.

(E) Correlation coefficient of spontaneous activity between neurons as a function of the distance between them; dashed line indicates unpaired mice; solid line indicates paired mice.

Note the lack of a significant difference in (C)–(E). Statistical analysis in (C) and (D), Mann-Whitney test; in (E) two-way ANOVA. Plots are mean  $\pm$  SEM. See also [Movie S2](#).

in a given trial. The pool of neurons recruited to encode a stimulus across trials is therefore significantly larger than the pool responding to a single stimulus.

Relative to explicitly unpaired controls, fear-conditioned mice exhibited significant reductions in both the fraction of neurons recruited across trials to encode the CS as well as the fraction of neurons responding to a single stimulus. When we used the average magnitude of spontaneous activity to define response threshold, we found that 38% fewer neurons responded to whisker stimulation when the CS predicted a foot shock compared to controls, (Figure 5A paired  $42.6\% \pm 4.6\%$ ; unpaired  $68.4\% \pm 6\%$ ,  $p = 0.0011$ ). Similarly, 34% fewer neurons responded to the CS relative to unpaired controls when the

threshold was based on the fidelity of spontaneous activity (Figure 5B, paired  $34.4\% \pm 4.0\%$ ; unpaired  $52.07\% \pm 5.3\%$ ,  $p = 0.013$ ). These thresholds, therefore, provide effectively the same value, and both show that, relative to controls, associative learning decreases the pool of neurons used to encode the CS across trials.

Fear conditioning also decreased the fraction of neurons responding to a single trial by 38% relative to controls (Figure 5C, paired:  $23\% \pm 3\%$ , unpaired:  $37\% \pm 4\%$ ,  $p = 0.029$ ). These measures of fractional response to a single trial are consistent with previous reports in anesthetized mice (Kerr et al., 2007; Sato et al., 2007) but see Crochet et al. (2011) in awake. Taken together, our data show that fear conditioning enhances sparse population coding of the CS in primary somatosensory cortex.

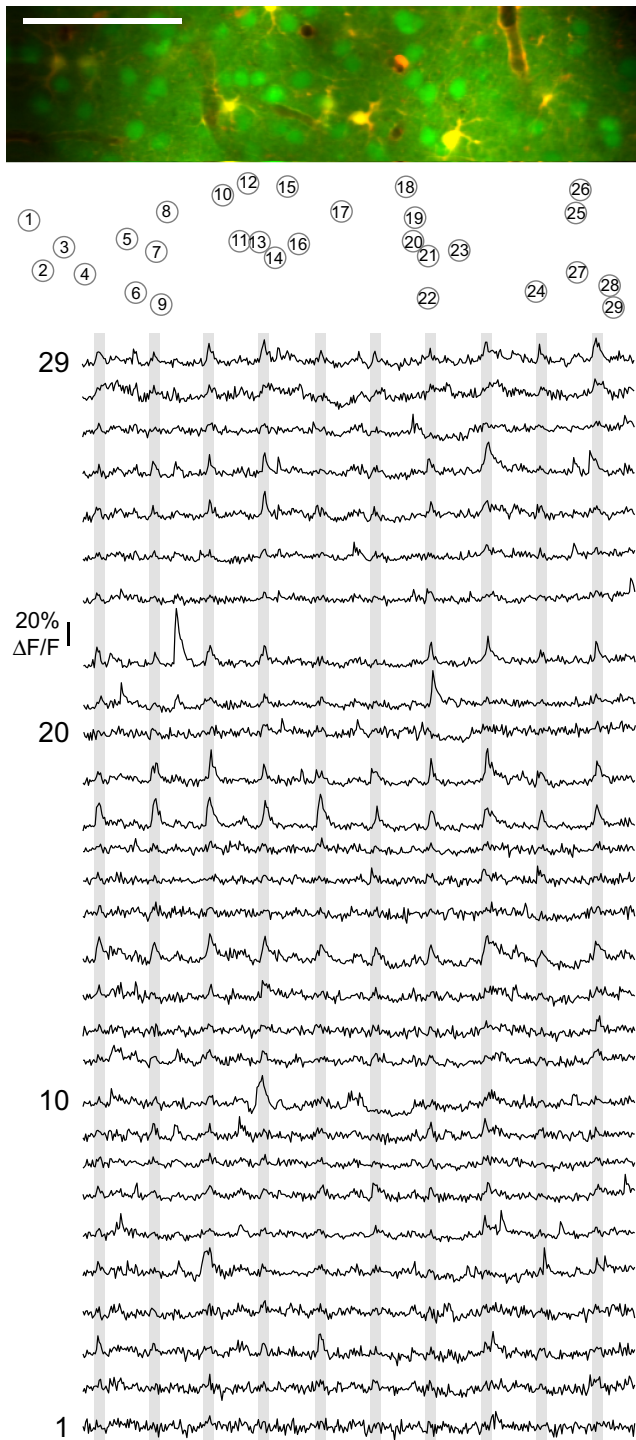


**Figure 4. Example of Evoked Responses**

A typical image of labeled cortical neurons, imaged *in vivo* with 2-photon excitation. OGB-1 labeling is green; SR101 labeling, which labels astrocytes, is red and the overlap is yellow. Scale bar: 50  $\mu\text{m}$ . The numbered circles below the image identify each of the neurons whose responses are shown. The numbers in the circles correspond to the numbered traces (cells 1, 10, and 20 are labeled to the left of the traces). The vertical gray lines delineate the time of whisker stimulation. Each trace is 120 s.

See also [Movie S3](#).

### Associative Fear Learning Increases Response Strength without Altering Response Fidelity

Associative learning did not alter response fidelity (Figure 5D right, paired 7.04; unpaired 7.12,  $p = 0.3914$ ), but did significantly increase the strength of response to the CS. The enhanced response was seen both when response magnitude was averaged across all trials, inclusive of failures (Figure 5E left paired  $6.33\% \pm 0.26\%$ ; unpaired  $5.31\% \pm 0.14\%$ ,  $dF/F$ ,  $p < 0.0001$ ) and when failures were excluded (Figure 5E right paired  $10.39\% \pm 0.30\%$ ; unpaired  $8.95\% \pm 1.80\%$   $dF/F$ ,  $p < 0.0001$ ).

We next plotted response magnitude as a function of response fidelity (Figure 5F) to examine whether there was an interaction effect between training and fidelity. Although there was no interaction (ANOVA  $F[5, 658] = 1.75$ ,  $p = 0.12$ ), there was a significant effect of fidelity on response magnitude for both paired and explicitly unpaired groups (ANOVA  $F[5, 658] = 58.02$ ,  $p < 0.001$ ), indicating that neurons with the highest response fidelity had stronger responses to each stimulus than neurons responding at lower fidelities.

To examine the effect of associative learning on total network activity we plotted the fraction of neurons in the total population as a function of their mean magnitude of fluorescent change (Figure 5G). This plot includes all neurons, whether responsive or not, and averages their responses across all ten trials, inclusive of failures. This plot thus provides a view of total cortical activity in layer 2/3. We found a small, but significant decrease (8%) in mean cortical response to whisker stimulation after fear learning (Figure 5G paired  $3.9 \pm 0.1$ , unpaired  $4.2\% \pm 0.1\%$   $dF/F$ ,  $p < 0.001$ ). This finding is in agreement with others (Castro-Alamanos, 2004; Jasinska et al., 2010; Kinoshita et al., 2009; Otazu et al., 2009; Polley et al., 1999).

Taken together, results from the associative learning procedure show that fear learning reduces the fraction of neurons responding to the CS, while increasing the strength of responsive neurons. The net effect is an enhancement of sparse population coding with a moderate decrease in total activity.

### Nonassociative Training Reduces Response Strength and Enhances Response Fidelity, but Does Not Affect Sparse Population Coding

Exposure to a nonreinforced stimulus results in nonassociative plasticity in primary sensory cortices (Dinse et al., 2003; Frenkel et al., 2006; Gilbert, 1998; Jasinska et al., 2010; Mégevand et al., 2009; Melzer and Steiner, 1997), and this has been proposed to be a substrate for perceptual learning (Frenkel et al., 2006). We used this form of nonassociative learning to examine if the effects observed after associative fear conditioning were general to learning per se, or were specific to associative fear learning. We measured population responses to whisker stimulation in mice exposed 4–5 days earlier to five CS presentations during a single trial with no US (five mice total of 520 neurons). Hereafter, we refer to this group as “stimulated.” Mice not exposed to the CS were used as controls (eight mice total of 789 neurons); hereafter, we refer to this group as “naive.”

Measures of spontaneous activity and network synchrony were not significantly different between naive and stimulated mice (Figure 6A, magnitude of fluorescent change: naive  $1.15\% \pm 0.03\%$ ; stimulated  $1.16\% \pm 0.04\%$   $dF/F$ ,  $p = 0.28$ ;

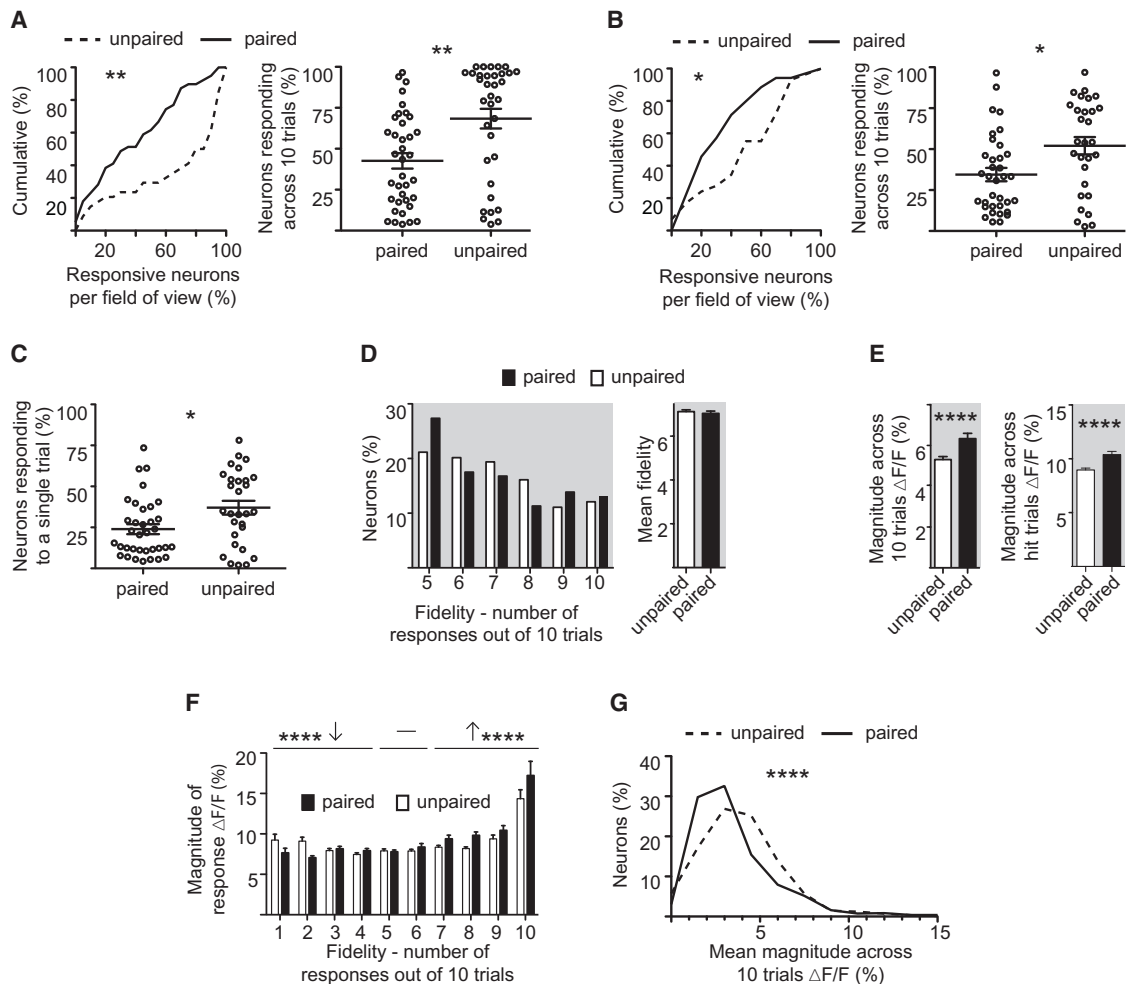


**Figure 5. Associative Fear Learning Increases Both Sparse Population Coding and Response Strength**

(A) (left) Cumulative percentage of responding neurons across trials per field of view in paired (solid line) or unpaired (dashed line) mice. Responsive neurons were defined based on mean fluorescent change across ten trials. (right) Fractional response per field of view in paired and unpaired mice. Note the decreased fractional response after learning.

(B) As in (A), but defining responsive neurons based on fidelity.

(C) Percentage of responsive neurons to a single stimulus trial per field of view in paired and unpaired mice.

(D) Percentage of responding neurons (defined as in B) plotted as a function of fidelity (left), and averaged fidelity (right). Note the absence of any significant change between paired (black bars) and unpaired (white bars) mice.

(E) Mean fluorescence change of responding neurons measured in unpaired (white bars) and paired (black bars) mice across all ten trials (left) or exclusive of failures (right). Note the significant increase in the paired group.

(F) Mean response magnitude as a function of fidelity, exclusive of failures, for responsive neurons in paired (black bars) or unpaired (white bars) mice.

(G) Percentage of neurons, responsive and not, plotted as a function of their mean response magnitude, inclusive of failures, for paired (solid line) and unpaired (dashed line) mice. Note the reduction in the paired group.

\* $p < 0.05$ , \*\* $p < 0.01$ , \*\*\* $p < 0.001$ , \*\*\*\* $p < 0.0001$ . Statistical analysis, (A)–(G): Mann-Whitney test. Plots are mean  $\pm$  SEM.

See also Figure S1.

Figure 6B, sham fidelity: naive 1.56; stimulated 1.49,  $p = 0.28$ ; Figure 6C, network synchrony: two-way ANOVA training X distance indicated no training effect  $F[7, 320] = 0.81$ ,  $p = 0.58$ . As above, these measures were used to derive the 95% threshold to define responsive neurons across trials. These values for  $dF/F$  were 3.1% for the stimulated group and 3.3% for naive controls. The 95% threshold for measures based on fidelity was four responses to ten trials for both groups.

Mere exposure to a nonreinforced stimulus did not significantly alter the fraction of neurons responding to single-trial whisker stimulation (Figure 7A, naive =  $33\% \pm 4\%$ , stimulated =  $44\% \pm 6\%$ ,  $p = 0.29$ ). Nor were significant changes seen when we analyzed the fraction of neurons recruited across all ten trials, as described above (Figure 7B: naive =  $62\% \pm 4\%$ , stimulated =  $68\% \pm 6\%$ ,  $p = 0.56$ ; Figure 7C: naive =  $47\% \pm 4\%$ , stimulated =  $57\% \pm 7\%$ ,  $p = 0.26$ ).

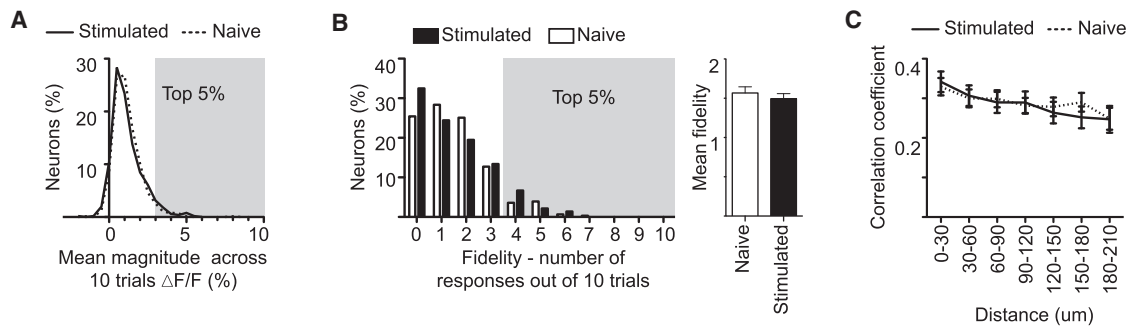


**Figure 6. Spontaneous Activity Is Unchanged by Nonassociative Learning**

(A) Percentage of neurons as a function of mean magnitude of fluorescent change time-locked to a sham stimulus. Dashed line indicates naive mice, solid line indicates whisker stimulated mice.

(B) (left) Percentage of neurons as a function of their fidelity—the number of times their spontaneous activity was time-locked to the sham stimuli. (right) Mean fidelity for each group. White bars indicate naive mice; black bars indicate stimulated mice. Gray shadings in (A) and (B) delineate the top 5% of neurons whose spontaneous activity was time-locked to a sham stimulus. This was subsequently used as a threshold to define evoked responsive neurons with 95% confidence. (C) Correlation coefficient between neurons as a function of the distance between them; dashed line indicates naive mice, and solid line indicates whisker stimulated mice.

Note the lack of a significant difference in (A)–(C) (statistical analysis A and B: Mann-Whitney test; C: two-way ANOVA). Plots are mean  $\pm$  SEM.

Notably, response fidelity, which was unaffected by associative fear learning, was strongly enhanced in stimulated mice (Figure 7D, naive 6.97, stimulated 8.28,  $p < 0.001$ ). Response magnitude, however, was reduced by stimulus exposure (Figure 7E, two-way ANOVA main effect of stimulation,  $F[1,1502] = 59.7$ ,  $p < 0.001$ ; means in bins 1–9 naive  $9.87\% \pm 0.16\%$ , stimulated  $8.31\% \pm 0.14\%$  dF/F). As in Figure 5F, there was a significant main effect of fidelity on response strength—in both the naive and stimulated groups, the neurons that responded with the highest fidelity (ten out of ten trials) had the largest changes in fluorescence (Figure 7E,  $F[9,1502] = 27.95$ ,  $p < 0.001$ ).

To examine the effect of passive stimulation on total network activity, we plotted the fraction of neurons in the total population as a function of their mean magnitude of fluorescent change (Figure 7F). Exposure to a nonreinforced stimulus increased total activity by 32.5% (failures included) relative to naive controls (Figure 7F, naive dF/F =  $4.64\% \pm 0.13\%$ , stimulated dF/F =  $6.15\% \pm 0.24\%$ ;  $p < 0.0001$ ).

Taken together, our data indicate that exposure to a nonreinforced stimulus has no effect on population sparsification, but does enhance response fidelity at the expense of response strength.

## DISCUSSION

### Summary

The goal of this study was to determine how associative fear learning shapes the local population response to the associated conditional stimulus in primary sensory cortex. To do this, we developed a paradigm in which controlled whisker stimulation in freely exploring mice could be paired with a foot shock. Mice in which foot shock was paired with whisker stimulation learned the association between the two stimuli and retained the memory for weeks, and possibly longer. This learning was reflected in the neural responses in the region of barrel cortex

mapping the trained whisker. Fewer neurons responded to stimulation of the trained whisker, yet their responses were stronger than those in control mice in which whisker stimulation was explicitly unpaired with foot shock. The emergence of sparse population coding and increased response strength after learning likely improves the metabolic efficiency of cortical processing. The increase in response strength improves robustness in terms of signal to noise, but is metabolically expensive. The enhanced sparsification of the population response likely compensates for the increased metabolic demand of the improved robustness, while simultaneously decreasing network crosstalk (Olshausen and Field, 2004). Supporting this view, we found that net activity—the average activity across all neurons, inclusive of failures—was reduced after associative fear learning.

Importantly, these changes were unique to associative learning. In mice that were merely exposed to the CS, response fidelity increased, but the strength of a given neuron's response decreased. The decreased robustness seen after CS exposure would likely compromise efficient stimulus encoding and may be responsible for the delayed encoding or latent inhibition that occurs with CS pre-exposure (Lubow and Moore, 1959). An enhancement of cortical response after the mere exposure to a salient stimulus has been observed before in primary cortices but the underlying neuronal correlate remained elusive (Dinse et al., 2003; Frenkel et al., 2006; Gilbert, 1998; Jasinska et al., 2010; Mégevand et al., 2009; Melzer and Steiner, 1997). We show that this increase is due to enhanced response fidelity. We did not observe such enhancement in mice exposed to the unpaired protocol. Therefore it appears that US presentation suppresses these nonassociative cortical changes. In Figure S1, we plot evoked responses for all four groups.

Taken together, these data support a model in which sparse network coding emerges in sensory cortex as the emotional significance of a stimulus is learned. Sparse coding is enabled by the overrepresentation of thalamic input in primary cortices, by a factor of up to 25 (Chalupa and Werner, 2003). This

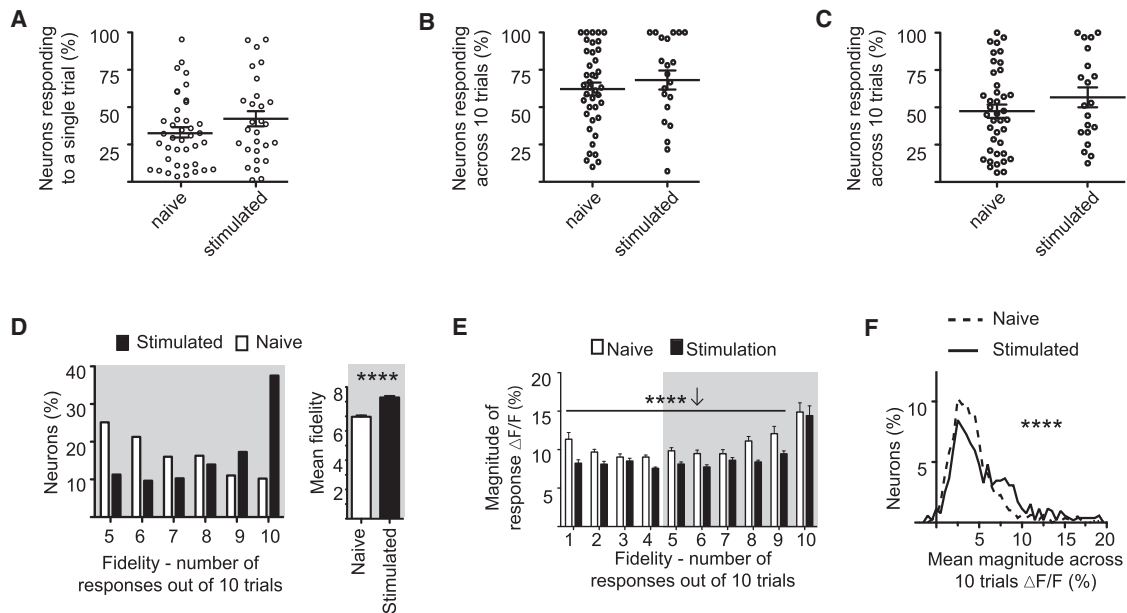


**Figure 7. Effects of Nonassociative Training on Cortical Network Responses**

(A) Percentage of responsive neurons to a single stimulus trial per field of view in stimulated and naive mice. Note the absence of any significant change between the two groups.

(B) Fraction of neurons in each field of view responding across ten stimulation epochs. Neurons were scored as responsive based on change in fluorescence across ten trials. Note the absence of any significant difference between the two groups.

(C) Fraction of neurons in each field of view responding across ten stimulation epochs. Neurons were scored as responsive based on response fidelity across ten trials. Note the absence of any significant difference between the two groups.

(D) Percentage of responding neurons (defined as in C) plotted as a function of their fidelity (left), and their averaged fidelity (right). Note the increase in fidelity in the stimulated group.

(E) Mean response magnitude as a function of fidelity, exclusive of failures, for all neurons in stimulated (black bars) or naive (white bars) mice. Note the lower magnitude in the stimulated group across fidelities 1–9.

(F) Percentage of neurons, responsive and not, plotted as a function of their mean response magnitude, inclusive of failures, for stimulated (solid line) and naive (dashed line) mice. Note the reduction in the naive group.

(\* $p < 0.05$ , \*\* $p < 0.01$ , \*\*\* $p < 0.001$ , \*\*\*\* $p < 0.0001$ ; statistical analysis, A–F: Mann-Whitney test). Plots are mean  $\pm$  SEM.

See also Figure S1.

magnification has been proposed to enable primary cortices to allocate neurons to represent associative attributes of a stimulus (Chalupa and Werner, 2003; Olshausen and Field, 2004), thereby improving the speed of sensory processing while reducing attention load (Hochstein and Ahissar, 2002; Olshausen and Field, 2004). In support of this model, behavioral studies suggest that after conditioning, although animals respond to the CS automatically, it commands reduced attention and processing (Bouton, 2007; Pearce and Hall, 1980). Although we did not directly study attention and automaticity, our findings provide empirical support for this type of model.

### Single Cell Plasticity after Learning

Our studies examined neural response distribution in the local network 4–5 days after mice were exposed to an associative learning paradigm. We do not know the time course over which the observed sparsification of the population response or the strengthening of neural responses emerges after pairing. However, receptive field plasticity following learning is known to develop rapidly within five trials in a single session (Edeline et al., 1993), and is fully expressed within 3 days post training

(Galván and Weinberger, 2002). The mechanisms driving this plasticity have been extensively studied in paradigms in which a stimulus is paired with a reinforcer, or with release of neuro-modulators (Bakin and Weinberger, 1996; Bao et al., 2001; Kilgard and Merzenich, 1998). A recent study in auditory cortex, in which a tone was paired with nucleus basalis stimulation, found that a rapid loss of inhibition precedes and likely permits a shift in excitatory receptive field tuning (Froemke et al., 2007). These excitatory shifts are later consolidated by the re-emergence of strong inhibition, which again balances the ratio of excitation and inhibition in the circuit. Such receptive field changes persist for at least 8 weeks, and quite possibly for the lifetime of the animal (Weinberger et al., 1993). However, our finding that a subset of neurons becomes more responsive even as the network response becomes sparser indicates that any inhibitory plasticity is not uniform across the local cortical network.

### Cortical Map Plasticity after Learning

Cortical map expansion is often observed after intense training. While learning-induced receptive field plasticity may occur in its

absence (Berlau and Weinberger, 2008; Kilgard et al., 2001), cortical map expansion enhances learning, and its reversal impairs memory (Reed et al., 2011). The expansion of the representation of the CS in a cortical map is driven by the strategy employed by the animal. If the onset of the stimulus is used as a cue, the cortical representation of the stimulus expands, but if behavior is cued by stimulus offset it does not (Bieszczad and Weinberger, 2010) [and see Polley et al., 1999] for bidirectional map plasticity). In addition, the magnitude of cortical map plasticity is proportional to the level of motivation (Rutkowski and Weinberger, 2005), which cannot be measured in our task. Though map plasticity enhances learning, recent findings indicate that it is transient (Molina-Luna et al., 2008; Reed et al., 2011; Yotsumoto et al., 2008). These findings indicate that the role of map plasticity may be to identify the minimum number of neurons required to achieve any given task. In this view, map expansion has two phases—the first of which involves a transient expansion of the pool of neurons that respond to the trained stimulus, and the second involving a selection of the most efficient circuitry from this enlarged pool (Reed et al., 2011). The result is a transient expansion of the map as neurons are recruited by the training, followed by a contraction to baseline as efficient, sparser coding is achieved. Although our experiment was not designed to detect different phases after learning, the increase sparsification that we observed after learning is in line with the prediction of this model. Our findings also suggest that after the second phase, the neuronal pool left responding to the stimulus is even smaller than the initial pool.

### Laminar Plasticity after Learning

Laminar plasticity of neural responses in adult somatosensory cortex has been extensively studied in mice and rats that have had all or a subset of whiskers removed (for review, see Feldman and Brecht, 2005). Emergent from these studies is a view of cortex in which layer 4, the primary recipient of thalamic input to cortex is highly plastic in very young mice but gradually loses plasticity during puberty, whereas layer 2/3 remains extensively and rapidly plastic in adults. Our observations after learning were limited to neurons in layer 2/3, and thus we do not know whether similar changes are seen in layer 4, or whether changes in layer 4 follow a similar time course.

### A Unique Role for High Fidelity Neurons in Learning?

In all groups examined, we found that the subset of neurons characterized by highest fidelity (those that respond >90% of the time that a stimulus is delivered) had larger fluorescent changes per response (exclusive of failures) than neurons responding with lower fidelity, indicating that these neurons respond with higher firing rates. Nonreinforced stimulus exposure dramatically increased this neuronal pool (Figure 7D) demonstrating that this pool is (at least) not exclusively composed of interneurons whose fraction in the population cannot be changed (see also Yassin et al., 2010). To our knowledge, such a pool has not been previously identified. We do not know what role this pool of neurons plays in cortical processing, but their disproportional contribution to the overall spike number suggests a unique role in encoding information.

## EXPERIMENTAL PROCEDURES

All procedures involving the handling and use of mice for these experiments were approved by the University of California Los Angeles Office for Protection of Research Subjects and the Chancellor's Animal Research Committee.

### Behavior

Mice (C57BL/6, Charles River) 9–10 weeks old were gradually habituated to the training context, to have a small metallic grain on their whisker, and to wear a custom-made Elizabethan collar (BrainTree), which prevented them from removing the metal, or the whisker. Habituation lasted 12 days as following: handling 2 days, 3 days of 1 hr exposure to the training context, 2 days of 1 hr with the collar in a regular clean cage, and 1 hr in the training context, 2 days with the collar in the training context, and 3 days with the collar, and with a metallic grain (length ~1.5 mm, diameter 0.2 mm) on the whisker inside the training context. The metallic grain was attached to the whisker with VetBond, and detached with Acetone, both under Isoflurane anesthesia.

FreezeFrame software (Coulbourn Instruments) controlled video recording of the mouse behavior (four frames/s), the delivery of a scrambled foot shock (MedAssociates) (0.6 mA 1.5 s), and the delivery of the CS (30 s, 8 Hz), which was generated by a 75 Gauss magnetic field. The voltage delivered to the electromagnet was adjusted with a transformer (Variatc SRV-20, Chuan Hsin) and the frequency was adjusted with a custom made unit (Critical Velocity). Training was done in a sound isolation box.

Mice received five CS presentations during a single trial that lasted 30 min. For paired mice, the US was given at the end of each CS. The mean intertrial interval (ITI) was 3 min beginning at the eighth minute. For unpaired mice, five USs with a mean ITI of 3 min were given beginning at the third minute, and five CSs were given with a mean ITI of 2.5 min beginning at the 16th minute. Mice trained with stimulation only received the paired procedure but no US.

Learning was tested in a modified context. The mice were placed in a tube with a plastic floor, and with some clean bedding. The tube was then inserted into the bore of the electromagnet. After 4 min, four CSs were presented with an ITI of 3 min. Freezing (lack of motion except breathing for 3 s) was scored by FreezeView software (Coulbourn Instruments). Baseline freezing was 2 min prior to the first CS. CS freezing was calculated using the mean of the four CS presentations for each mouse. The significance of the variation during the CS presentation or during baseline was tested using a one-way ANOVA followed by Tukey's posttest or, if there were only two groups, a *t* test.

### Cranial Window for Optical Imaging

Carprofen (Pfizer 15 µg/25 g mouse) analgesia was administered subcutaneously prior to surgery and then daily for the next 4 days. Mice were anesthetized with Isoflurane (5% for induction, 1%–2% thereafter), the scalp and connective tissue were removed, and the dry skull was covered with VetBond. An aluminum metal bar with two traded holes was attached to the skull with black Dental Acrylic. A 3-mm-diameter craniotomy was done above the barrel cortex (from Bregma: rostral –1.5, lateral 3 mm). A custom-made 3 mm cover-glass (Bellco Glass) was placed and sealed with VetBond cyanoacrylate glue. The dry glue was covered with Dental Acrylic. Ringer solution (1 ml) was given subcutaneous after the surgery. During the surgery, and until full recovery, the mouse temperature was kept at 37°C using a heated plate and a rectal temperature sensor.

### Intrinsic Signal Optical Imaging

Mice with cranial window for chronic imaging (Holtmaat et al., 2009) or with thinned skull for acute imaging were sedated with 10 mg/kg Chlorprothixene (Sigma) in DMSO, and anesthetized with isoflurane (5% for induction, 0.6% thereafter) in pure oxygen. The mice were mounted in a custom-made stage using a preattached head bar, and their temperature was kept on 37°C using a heated plate and a rectal temperature sensor. Two 30 awg (Magnetic Sensor Systems) metal wires were glued to whiskers C1 and E2. The whiskers were inserted into two glass pipettes attached to two piezo actuators (Piezo Systems), which were controlled by a Master8 device (A.M.P.I. Israel). A function generator (BK Precision) converted the square signal from the Master8 into 0.7 Amp saw-tooth signal, which was then amplified 20× and delivered to the piezo. This generated whisker movement of about 2°. Alternate runs

of the two whiskers were done; in each, only one whisker was stimulated (five deflections every 8 s). At the same time, the barrel cortex was illuminated with 630 nm light. The reflected light was collected through 630 nm filter placed before a tandem lens microscope consisting of 35 and 135 mm focal length F-mount photographic lenses (Nikon), providing a 3.9× magnification. The microscope was focused 500 μm beneath the cortical surface. Movies (8 min) were acquired at 30 frames per second using a 12 bit charge-coupled device camera (Dalsa 1M30), a frame grabber (Matrox Meteor II/Dig), and custom software. To achieve image depth of 16 bits, frames were binned four times temporally and 2 × 2 spatially. To reduce slow general effects on light reflection, the row light reflection values were converted into reflection changes between adjacent frames:  $(R - R_0)/R$  when R was the reflection acquired in a pixel x in frame n, and  $R_0$  was R for frame n-1. Fourier analysis of the resulting vector across the run in each pixel isolated the component of the signal that matched the frequency of the stimulation (0.125 Hz) (Kalatsky and Stryker, 2003). The square power of that was then assigned to that pixel. When applied to all pixels this generated a map on which the barrel was easily identified, and was further enhanced by using a 5 × 5 Gaussian filter.

### Electroencephalographic Recordings

Mice were implanted with two monopolar surface electrodes placed over the right barrel cortex and the cerebellum was used as reference. Electrodes made of stainless-steel wire isolated by polyester (diameter, 0.125 mm; FE245840; Goodfellow), were inserted between the skull and the dura then maintained by dental cement. Electroencephalographic (EEG) signals were amplified, filtered (1,000×, bandpass 0.1 Hz to 3 kHz; Model 3000; AM-Systems, Inc), and stored to hard disk (sampling rate: 1,240 Hz. NIDAQ-MX/BNC-2090[SE], National Instrument) using WinEDR software (Strathclyde Electrophysiology Software, Strathclyde University). Mice were simultaneously filmed during the recording using a Logitech Carl Zeiss Tessar HD 1080p camera. Time frequency analysis was performed using sliding (87.5% overlap) fast Fourier transform after Hanning window using the Igor sonogram function.

### Ca Imaging

Mice were prepared as for “cranial window,” but instead of removing the skull, it was thinned enough to see the small blood vessels. Ultra low-temperature melting Agarose (USB) was applied on top of the skull and covered with a 1.2 cm cover glass (Fisherbrand). We found ultra low-temperature melting Agarose crucial for success. The location of the barrel was identified with intrinsic-signal optical imaging. A 3 mm craniotomy was then made to encompass the identified barrel.

Cell populations were labeled in superficial neocortical layers with the calcium indicator Oregon Green BAPTA-1 (OGB-1, Invitrogen) mixed with Sulforhodamine-101 (Sigma) (Nimmerjahn et al., 2004) using the multicell bolus loading technique (Stosiek et al., 2003). Briefly, 50 μg of the membrane-permeant acetoxymethyl (AM) ester form of OGB-1 were dissolved in 4 μl DMSO/20% Pluronic F-127 (Invitrogen) and diluted 13 times with dye buffer (150 mM NaCl, 2.5 mM KCl, 10 mM HEPES [pH 7.4]) and with 1.5 μl Sulforhodamine (1 mM) to a final concentration of about 1 mM. The dye was delivered in depth of 250 microns through 4 MΩ glass pipettes over 1 min with a pressure of 10 PSI using a Picospritzer. After injections, the cranial window was sealed as described earlier.

The mice were sedated and kept with 0.25%–0.4% Isoflurane. EEG recordings indicated that mice remained in a slow-wave EEG pattern for the entirety of the recording session. Video recording showed that whisker twitching was absent in the sedated mice over this period. Imaging was done in depth of 200–250 μm under the Dura using 4 Hz line scan (wavelength 870 nm) using a custom made 2-photon microscope with a 40× objective (Zeiss, 1.0 NA). The emitted red and green light was separated using a dichroic mirror (Semrock) and collected by two photomultiplier tubes (Hamamatsu R3896). Whisker deflection was triggered by the microscope operating system, Scan-Image (Pologruto et al., 2003), to allow synchronization. Custom code was used to generate a sine wave, which was then amplified and delivered to a piezo actuator. The piezoelectric stimulator was positioned approximately 5 mm from the base of the whisker. Each whisker stimulation epoch consisted of a 5 Hz, 20V signal delivered to the piezo actuator, resulting in a deflection of approximately 400 μm. Each of the five stimuli comprising the stimulus was

25 ms in duration peak-to-peak. In each imaging trial there were ten epochs of 5 Hz whisker stimulation, each 10 s apart.

Neurons were distinguished from astrocytes using Sulforhodamine coinjection (Nimmerjahn et al., 2004). Analysis of the data was similar to (Mrsic-Flogel et al., 2007). All neurons in a field of view were identified using a semiautomated custom made routines (Matlab). In each trial, the fluorescence observed during a 2 s time prior to the stimulation was defined as a baseline ( $F_0$ ). The change of fluorescence in each frame (F) from baseline was calculated as:  $(F - F_0)/F_0$ . Then, the averaged trace of all ten trials was calculated. A response window was defined from the initiation of the stimulation until 1 s post.

Response to a single trial was defined by three parameters: (1) a fluorescent change of at least 5% above the baseline preceding this trial that corresponds to one spike (Ch'ng and Reid, 2010); (2) a fluorescent change greater than the mean plus three SDs calculated from a baseline derived from the 2 s preceding each of the ten trials (this baseline was computed from the median of each time point across all ten trials to reduce the effect of spontaneous spikes during baseline); and (3) at least a 3% increase in fluorescence from the former frame to the peak-response frame in the 2 s response window to reflect fast rise time of the signal (Greenberg et al., 2008). Responsive neurons across trials were defined based on two measure of spontaneous activity.

### Statistical Analysis

Statistical analysis consisted of the following: t test (Figures 1C and 1D), one-way ANOVA, Tukey's post-hoc test (Figures 2A–2C), Mann-Whitney nonparametric test (Figures 3C, 3D, 5A–5G, 6A, 6B, 7A–7D, and 7F), and two-way ANOVA (Figures 3E and 6C training × distance), (Figures 5F and 7E training × fidelity).

### SUPPLEMENTAL INFORMATION

Supplemental Information includes one figure and three movies and can be found with this article online at <http://dx.doi.org/10.1016/j.neuron.2012.04.035>.

### ACKNOWLEDGMENTS

This work was funded by grants from the National Institute of Mental Health to J.T.T. (P50MH077972 and R01MH082935), M.S.F. (R01MH062122), and A.J.S. (P50MH077972). We thank M. Stryker, D. Buonomano, and A. Matynia for their helpful comments on earlier versions of the manuscript; R. Edelshtein for help with video editing; J. Friedman, B. Jayaprakash, and G. Arom for help with electronics; and G.W. Byeon, A. Pyo, W. Columna, and G. Evans for help in behavior.

Accepted: April 20, 2012

Published: July 11, 2012

### REFERENCES

- Attwell, D., and Laughlin, S.B. (2001). An energy budget for signaling in the grey matter of the brain. *J. Cereb. Blood Flow Metab.* 21, 1133–1145.
- Bakin, J.S., and Weinberger, N.M. (1996). Induction of a physiological memory in the cerebral cortex by stimulation of the nucleus basalis. *Proc. Natl. Acad. Sci. USA* 93, 11219–11224.
- Bao, S., Chan, V.T., and Merzenich, M.M. (2001). Cortical remodelling induced by activity of ventral tegmental dopamine neurons. *Nature* 412, 79–83.
- Berlau, K.M., and Weinberger, N.M. (2008). Learning strategy determines auditory cortical plasticity. *Neurobiol. Learn. Mem.* 89, 153–166.
- Bieszczad, K.M., and Weinberger, N.M. (2010). Remodeling the cortex in memory: Increased use of a learning strategy increases the representational area of relevant acoustic cues. *Neurobiol. Learn. Mem.* 94, 127–144.
- Bouton, M.E. (2007). *Learning and Behavior: A Contemporary Synthesis* (Sunderland, MA: Sinauer Associates Inc.).
- Castro-Alamancos, M.A. (2004). Absence of rapid sensory adaptation in neocortex during information processing states. *Neuron* 41, 455–464.

- Chalupa, L.M., and Werner, J.S. (2003). *The Visual Neurosciences* (Cambridge, MA: MIT Press).
- Ch'ng, Y.H., and Reid, R.C. (2010). Cellular imaging of visual cortex reveals the spatial and functional organization of spontaneous activity. *Front. Integr. Neurosci.* 4.
- Crochet, S., Poulet, J.F., Kremer, Y., and Petersen, C.C. (2011). Synaptic mechanisms underlying sparse coding of active touch. *Neuron* 69, 1160–1175.
- Das, S., Weiss, C., and Disterhoft, J.F. (2001). Eyeblink conditioning in the rabbit (*Oryctolagus cuniculus*) with stimulation of the mystacial vibrissae as a conditioned stimulus. *Behav. Neurosci.* 115, 731–736.
- Dinse, H.R., Ragert, P., Pleger, B., Schwenkreis, P., and Tegenthoff, M. (2003). Pharmacological modulation of perceptual learning and associated cortical reorganization. *Science* 301, 91–94.
- Edeline, J.M., Pham, P., and Weinberger, N.M. (1993). Rapid development of learning-induced receptive field plasticity in the auditory cortex. *Behav. Neurosci.* 107, 539–551.
- Fanselow, M.S., and Bolles, R.C. (1979). Naloxone and shock-elicited freezing in the rat. *J. Comp. Physiol. Psychol.* 93, 736–744.
- Feldman, D.E., and Brecht, M. (2005). Map plasticity in somatosensory cortex. *Science* 310, 810–815.
- Frenkel, M.Y., Sawtell, N.B., Diogo, A.C., Yoon, B., Neve, R.L., and Bear, M.F. (2006). Instructive effect of visual experience in mouse visual cortex. *Neuron* 51, 339–349.
- Froemke, R.C., Merzenich, M.M., and Schreiner, C.E. (2007). A synaptic memory trace for cortical receptive field plasticity. *Nature* 450, 425–429.
- Gale, G.D., Anagnostaras, S.G., Godsil, B.P., Mitchell, S., Nozawa, T., Sage, J.R., Wiltgen, B., and Fanselow, M.S. (2004). Role of the basolateral amygdala in the storage of fear memories across the adult lifetime of rats. *J. Neurosci.* 24, 3810–3815.
- Galván, V.V., and Weinberger, N.M. (2002). Long-term consolidation and retention of learning-induced tuning plasticity in the auditory cortex of the guinea pig. *Neurobiol. Learn. Mem.* 77, 78–108.
- Galvez, R., Weiss, C., Weible, A.P., and Disterhoft, J.F. (2006). Vibrissa-signaled eyeblink conditioning induces somatosensory cortical plasticity. *J. Neurosci.* 26, 6062–6068.
- Galvez, R., Weible, A.P., and Disterhoft, J.F. (2007). Cortical barrel lesions impair whisker-CS trace eyeblink conditioning. *Learn. Mem.* 14, 94–100.
- Galvez, R., Weiss, C., Cua, S., and Disterhoft, J. (2009). A novel method for precisely timed stimulation of mouse whiskers in a freely moving preparation: application for delivery of the conditioned stimulus in trace eyeblink conditioning. *J. Neurosci. Methods* 177, 434–439.
- Garaschuk, O., Milos, R.I., and Konnerth, A. (2006). Targeted bulk-loading of fluorescent indicators for two-photon brain imaging in vivo. *Nat. Protoc.* 1, 380–386.
- Gilbert, C.D. (1998). Adult cortical dynamics. *Physiol. Rev.* 78, 467–485.
- Golshani, P., Gonçalves, J.T., Khoshkoo, S., Mostany, R., Smirnakis, S., and Portera-Cailliau, C. (2009). Internally mediated developmental desynchronization of neocortical network activity. *J. Neurosci.* 29, 10890–10899.
- Greenberg, D.S., Houweling, A.R., and Kerr, J.N. (2008). Population imaging of ongoing neuronal activity in the visual cortex of awake rats. *Nat. Neurosci.* 11, 749–751.
- Grinvald, A., Lieke, E., Frostig, R.D., Gilbert, C.D., and Wiesel, T.N. (1986). Functional architecture of cortex revealed by optical imaging of intrinsic signals. *Nature* 324, 361–364.
- Harris, J.A., Petersen, R.S., and Diamond, M.E. (1999). Distribution of tactile learning and its neural basis. *Proc. Natl. Acad. Sci. USA* 96, 7587–7591.
- Hochstein, S., and Ahissar, M. (2002). View from the top: hierarchies and reverse hierarchies in the visual system. *Neuron* 36, 791–804.
- Holtmaat, A., Bonhoeffer, T., Chow, D.K., Chuckowree, J., De Paola, V., Hofer, S.B., Hübener, M., Keck, T., Knott, G., Lee, W.C., et al. (2009). Long-term, high-resolution imaging in the mouse neocortex through a chronic cranial window. *Nat. Protoc.* 4, 1128–1144.
- Houweling, A.R., and Brecht, M. (2008). Behavioural report of single neuron stimulation in somatosensory cortex. *Nature* 451, 65–68.
- Huber, D., Petreanu, L., Ghilani, N., Ranade, S., Hromádka, T., Mainen, Z., and Svoboda, K. (2008). Sparse optical microstimulation in barrel cortex drives learned behaviour in freely moving mice. *Nature* 451, 61–64.
- Jasinska, M., Siucinska, E., Cybulska-Klosowicz, A., Pyza, E., Furness, D.N., Kossut, M., and Glazewski, S. (2010). Rapid, learning-induced inhibitory synaptogenesis in murine barrel field. *J. Neurosci.* 30, 1176–1184.
- Kalatsky, V.A., and Stryker, M.P. (2003). New paradigm for optical imaging: temporally encoded maps of intrinsic signal. *Neuron* 38, 529–545.
- Kerr, J.N., de Kock, C.P., Greenberg, D.S., Bruno, R.M., Sakmann, B., and Helmchen, F. (2007). Spatial organization of neuronal population responses in layer 2/3 of rat barrel cortex. *J. Neurosci.* 27, 13316–13328.
- Kilgard, M.P., and Merzenich, M.M. (1998). Cortical map reorganization enabled by nucleus basalis activity. *Science* 279, 1714–1718.
- Kilgard, M.P., Pandya, P.K., Vazquez, J., Gehi, A., Schreiner, C.E., and Merzenich, M.M. (2001). Sensory input directs spatial and temporal plasticity in primary auditory cortex. *J. Neurophysiol.* 86, 326–338.
- Kim, J.J., and Fanselow, M.S. (1992). Modality-specific retrograde amnesia of fear. *Science* 256, 675–677.
- Kinoshita, M., Gilbert, C.D., and Das, A. (2009). Optical imaging of contextual interactions in V1 of the behaving monkey. *J. Neurophysiol.* 102, 1930–1944.
- Lubow, R.E., and Moore, A.U. (1959). Latent inhibition: the effect of nonreinforced pre-exposure to the conditional stimulus. *J. Comp. Physiol. Psychol.* 52, 415–419.
- Mégevand, P., Troncoso, E., Quairiaux, C., Muller, D., Michel, C.M., and Kiss, J.Z. (2009). Long-term plasticity in mouse sensorimotor circuits after rhythmic whisker stimulation. *J. Neurosci.* 29, 5326–5335.
- Melzer, P., and Steiner, H. (1997). Stimulus-dependent expression of immediate-early genes in rat somatosensory cortex. *J. Comp. Neurol.* 380, 145–153.
- Melzer, P., Van der Loos, H., Dörfel, J., Welker, E., Robert, P., Emery, D., and Berrini, J.C. (1985). A magnetic device to stimulate selected whiskers of freely moving or restrained small rodents: its application in a deoxyglucose study. *Brain Res.* 348, 229–240.
- Meyer, K., Kaplan, J.T., Essex, R., Webber, C., Damasio, H., and Damasio, A. (2010). Predicting visual stimuli on the basis of activity in auditory cortices. *Nat. Neurosci.* 13, 667–668.
- Molina-Luna, K., Hertler, B., Buitrago, M.M., and Luft, A.R. (2008). Motor learning transiently changes cortical somatotopy. *Neuroimage* 40, 1748–1754.
- Mrsic-Flogel, T.D., Hofer, S.B., Ohki, K., Reid, R.C., Bonhoeffer, T., and Hübener, M. (2007). Homeostatic regulation of eye-specific responses in visual cortex during ocular dominance plasticity. *Neuron* 54, 961–972.
- Nimmerjahn, A., Kirchhoff, F., Kerr, J.N., and Helmchen, F. (2004). Sulforhodamine 101 as a specific marker of astroglia in the neocortex in vivo. *Nat. Methods* 1, 31–37.
- O'Connor, D.H., Peron, S.P., Huber, D., and Svoboda, K. (2010). Neural activity in barrel cortex underlying vibrissa-based object localization in mice. *Neuron* 67, 1048–1061.
- Olshausen, B.A., and Field, D.J. (2004). Sparse coding of sensory inputs. *Curr. Opin. Neurobiol.* 14, 481–487.
- Otazu, G.H., Tai, L.H., Yang, Y., and Zador, A.M. (2009). Engaging in an auditory task suppresses responses in auditory cortex. *Nat. Neurosci.* 12, 646–654.
- Pearce, J.M., and Hall, G. (1980). A model for Pavlovian learning: variations in the effectiveness of conditioned but not of unconditioned stimuli. *Psychol. Rev.* 87, 532–552.
- Polley, D.B., Chen-Bee, C.H., and Frostig, R.D. (1999). Two directions of plasticity in the sensory-deprived adult cortex. *Neuron* 24, 623–637.
- Polley, D.B., Steinberg, E.E., and Merzenich, M.M. (2006). Perceptual learning directs auditory cortical map reorganization through top-down influences. *J. Neurosci.* 26, 4970–4982.

- Pologruto, T.A., Sabatini, B.L., and Svoboda, K. (2003). ScanImage: flexible software for operating laser scanning microscopes. *Biomed. Eng. Online* 2, 13.
- Recanzone, G.H., Schreiner, C.E., and Merzenich, M.M. (1993). Plasticity in the frequency representation of primary auditory cortex following discrimination training in adult owl monkeys. *J. Neurosci.* 13, 87–103.
- Reed, A., Riley, J., Carraway, R., Carrasco, A., Perez, C., Jakkamsetti, V., and Kilgard, M.P. (2011). Cortical map plasticity improves learning but is not necessary for improved performance. *Neuron* 70, 121–131.
- Rossettelet, C., Fieschi, M., Hugues, S., and Bureau, I. (2011). Associative learning changes the organization of functional excitatory circuits targeting the supragranular layers of mouse barrel cortex. *Front Neural Circuits* 4, 126.
- Rutkowski, R.G., and Weinberger, N.M. (2005). Encoding of learned importance of sound by magnitude of representational area in primary auditory cortex. *Proc. Natl. Acad. Sci. USA* 102, 13664–13669.
- Sato, T.R., Gray, N.W., Mainen, Z.F., and Svoboda, K. (2007). The functional microarchitecture of the mouse barrel cortex. *PLoS Biol.* 5, e189.
- Shuler, M.G., and Bear, M.F. (2006). Reward timing in the primary visual cortex. *Science* 311, 1606–1609.
- Siucinska, E., and Kossut, M. (1996). Short-lasting classical conditioning induces reversible changes of representational maps of vibrissae in mouse SI cortex—a 2DG study. *Cereb. Cortex* 6, 506–513.
- Stosiek, C., Garaschuk, O., Holthoff, K., and Konnerth, A. (2003). In vivo two-photon calcium imaging of neuronal networks. *Proc. Natl. Acad. Sci. USA* 100, 7319–7324.
- Vinje, W.E., and Gallant, J.L. (2000). Sparse coding and decorrelation in primary visual cortex during natural vision. *Science* 287, 1273–1276.
- Weinberger, N.M. (2004). Experience-dependent response plasticity in the auditory cortex: issues, characteristics, mechanisms, and functions. In *Plasticity of the Auditory System*, T.N. Parks, E.W. Rubel, R.R. Fay, and A.N. Popper, eds. (New York: Springer), pp. 173–227.
- Weinberger, N.M., Javid, R., and Lapan, B. (1993). Long-term retention of learning-induced receptive-field plasticity in the auditory cortex. *Proc. Natl. Acad. Sci. USA* 90, 2394–2398.
- Willmore, B.D., Mazer, J.A., and Gallant, J.L. (2011). Sparse coding in striate and extrastriate visual cortex. *J. Neurophysiol.* 105, 2907–2919.
- Yassin, L., Benedetti, B.L., Jouhannau, J.S., Wen, J.A., Poulet, J.F., and Barth, A.L. (2010). An embedded subnetwork of highly active neurons in the neocortex. *Neuron* 68, 1043–1050.
- Yotsumoto, Y., Watanabe, T., and Sasaki, Y. (2008). Different dynamics of performance and brain activation in the time course of perceptual learning. *Neuron* 57, 827–833.
- Zhou, X., de Villers-Sidani, E., Panizzutti, R., and Merzenich, M.M. (2010). Successive-signal biasing for a learned sound sequence. *Proc. Natl. Acad. Sci. USA* 107, 14839–14844.